TISSUE ENGINEERING: Part A
Volume 16, Number 9, 2010

DOI: 10.1089/ten.tea.2009.0635

Adipose Tissue Progenitor Cells Directly Interact with Endothelial Cells to Induce Vascular Network Formation

Stephanie Merfeld-Clauss, B.S.,[1,2] Nagesh Gollahalli, M.D.,[1,2]
Keith L. March, M.D., Ph.D.,[1–4] and Dmitry O. Traktuev, Ph.D.[1,2]

Adipose stromal cells (ASCs) express markers and functional properties of pericytes *in vitro* and, in combination with endothelial cells (ECs), are able to establish multilayer functional vessels *in vivo*. However, the factors that coordinate EC-ASC communications to promote migration of these cells toward one another, and their heterotypic assembly into vascular structures are not well defined. To understand the mechanisms of EC-ASC interaction, we developed an *in vitro* model of coculturing ECs with ASCs in a system containing serum but no additional exogenous cytokines or extracellular matrix (ECM) proteins. We demonstrated that ASCs have a profound potential to stimulate morphogenesis of ECs into branching networks of cord structures. The vascular networks developed in 6 days and were stable for at least 3 weeks. This process was associated with an increase in ECM protein production by ASCs and ECs, α-smooth muscle actin expression by ASCs, and increased CD31/platelet endothelial cell adhesion molecule-1 (PECAM-1) surface presentation by ECs. The vascular network formation (VNF) was dependent on matrix metalloproteinase activity and cell communications through vascular endothelial growth factor, hepatocyte growth factor, and platelet-derived growth factor-BB pathways. ASCs exhibited significantly higher potential to stimulate VNF than smooth muscle cells and fibroblasts. Media conditioned by ASCs promoted VNF by ECs cultured on smooth muscle cells and fibroblasts, but could not replace the presence of ASCs in coculture. The presence of ASCs in EC-fibroblast cocultures in a low fraction efficiently stimulated VNF. These findings demonstrate that the vasculogenesis-promoting potential of ASCs depends on interaction with ECs involving contact and likely bi-directional interaction, resulting in modulated secretion of cytokines and ECM proteins.

Introduction

Development of vascular networks that can sufficiently conduct blood flow to underperfused tissues is one of the major therapeutic goals for treating patients with ischemic disorders and for tissue engineering. Progenitor cell transplantation has emerged as a novel approach to improve tissue perfusion and stimulate functional tissue recovery. To date, numerous experimental models and clinical trials have focused on evaluating the angiogenic potential of various subtypes of blood-derived mononuclear cells, endothelial progenitor cells,[1–3] and bone marrow stem/stromal cells.[4–13]

It has been shown that endothelial colony forming cells,[14] a subtype of blood-derived endothelial progenitor cells, form functional vessels *in vivo* when implanted in mice[15]; however, the newly formed vessels were limited in frequency and size.[16] This finding agrees with prior observations demonstrating that mature endothelial cells (ECs) are able to establish only single-layer narrow-caliber vessels,[17] whereas genetic modification of ECs with bcl-2, which repressed EC apoptosis, led to formation of large-caliber, functional vessels with thick walls.[17]

We have hypothesized that the failure of nontransformed ECs to establish stable mature vasculature is related to the absence of a stabilizing layer of mural cells (e.g., pericytes and smooth muscle cells [SMCs]) in the time period immediately after implantation. The absence of this mural layer leads to degradation of the EC-formed small-caliber vessels, followed by EC apoptosis. This hypothesis is supported by a series of observations demonstrating that coimplantation of ECs with mesenchymal cells, such as human saphenous vein[18] and aortic[19] SMCs, as well as blood-derived[20] and bone marrow[16] mesenchymal stromal cells promoted *in vivo* formation of stable, functional vascular networks. However, the need for significant expansion to obtain adequate cell numbers for autologous therapies presents a potential limitation for use of mural cells from these sources.

Adipose stromal cells (ASCs), pluripotent cells derived from adipose tissue, represent a novel source of cells with

[1]Department of Medicine, [2]Indiana Center for Vascular Biology and Medicine, and [3]Department of Cellular and Integrative Physiology, Indiana University School of Medicine, Indianapolis, Indiana.
[4]R.L. Roudebush VA Medical Center, Indianapolis, Indiana.

significant potential for use in autologous cell therapies.[21] We have previously shown that in adipose tissue ASCs are predominantly localized in the peri-endothelial layer of the blood vessels, and are phenotypically and functionally equivalent to pericytes of microvessels.[22] We also demonstrated that human ASCs secrete a variety of bioactive molecules, including vascular endothelial growth factor (VEGF), hepatocyte growth factor (HGF), and granulocyte macrophage colony-stimulating factor (GM-CSF), which promote ECs survival[22] and proliferation.[23] Additionally, ASCs stabilize endothelial networks formed on the surface of Matrigel[22] by direct interaction with ECs. The robust vasculogenic potential of ASCs was further confirmed *in vivo* by coimplantation of ECs and ASCs into mouse tissue.[24] Despite these observations, the mechanisms governing the interactions between the ECs and ASCs (or other mural progenitor cells), and the parameters necessary for efficient and consistent vessel development are not well defined.

Formation of stable vessels is a complex process requiring finely orchestrated interactions between cells and the surrounding environment. These include temporal secretion of angiogenic factors, formation of an extracellular matrix (ECM), and cell proliferation and migration. The majority of the systems used for *in vitro* and *in vivo* studies of the angiogenic potential of cells are too complex (presence of ECMs and cytokines in the culture systems) to be suitable for initial analysis and identification of the interaction pathways between ECs and ASCs. Moreover, the presence of exogenous ECM proteins that are often used as an underlayer for cell culturing *in vitro* or as carrier in *in vitro* and *in vivo* models can significantly influence the behavior of the cells.

The system that was used in this study to evaluate the interactions between ASCs and ECs is a modified model of coculturing fibroblasts and ECs.[25,26] The present model is relatively free of exogenous factors, particularly ECM proteins and growth factors, instead relying on the factors produced by the ASCs and ECs in coculture.

Materials and Methods

All procedures for collecting human tissues (umbilical cord and adipose tissue) were approved by the Indiana University School of Medicine Institutional Review Board.

Isolation and culture of cells

Human adipose stromal cells. Human ASCs were isolated from human subcutaneous adipose tissue samples obtained from liposuction procedures as previously described.[22] Samples were obtained from 12 patients (11 healthy donors and 1 patient with diabetese) aged 27–57 years (36.9 ± 2.3) with body mass index 19–32 (25.6 ± 1.3). Briefly, samples were digested in collagenase type I solution (Worthington Biochemical) under agitation for 1 h at 37°C, and centrifuged at 300 *g* for 8 min to separate the stromal cell fraction (pellet) from adipocytes. The pellets were filtered through 250 μm Nitex filters (Sefar America, Inc.) and treated with red cell lysis buffer (154 mM NH_4Cl, 10 mM $KHCO_3$, and 0.1 mM ethylenediaminetetraacetic acid). The final pellet was resuspended and cultured in EGM-2mv (Cambrex). Monolayers of ASCs were passaged when 60%–80% confluent and used at passages 3–6. Purity of ASC samples from EC contamination was confirmed by staining ASC monolayers with anti-CD31 antibodies.

Cord-blood-derived endothelial cells. Cord-blood-derived (CBD) ECs were isolated from the umbilical cord vein blood of healthy newborns (38–40 weeks gestational age) as previously described.[14] Mononuclear cells were isolated from blood samples by gradient centrifugation through Histopaque 1077 (ICN), followed by culturing in the EGM-2/10% fetal bovine serum (FBS) (Cambrex) medium in six-well tissue culture plates (5×10^7 cells/well) precoated with type I rat tail collagen (BD Biosciences). The culture medium was changed daily for 7 days and then every other day until first passage. Confluent CBD-ECs were replated into flasks coated with type I rat tail collagen and cultured in the EGM-2/10% FBS medium. Cells were passaged after becoming 90% confluent and used at passages 4–6.

Other cells used in the study. All cells were purchased from Lonza (Allendale, NJ) and expanded and used at passages 5–7. Human coronary artery SMCs (CaSMCs) and human aortic SMCs (AoSMCs) were expanded in the SMGM-2 medium, normal human dermal fibroblasts (NHDFs) in FGM-2 or EGM-2mv, human umbilical vein ECs in EGM-2, and human microvascular ECs in EGM-2mv.

Coculture of ECs and ASCs

ASCs were plated on culture plastic at a density of 6×10^4 cells/cm^2 in the endothelial basal media (EBM)-2/5% FBS medium. In most of the experiments, ASCs were allowed to attach to the plates for 3 h, and then ECs from the indicated sources were plated on the top of ASC monolayer at densities ranging from 625 to 10,000 cells/cm^2. Cells were cultured in EBM-2/5% FBS for 6 days with medium change at day 3.

In a separate set of experiments, ASCs at 6×10^4 cells/cm^2 and CBD-ECs at 5×10^3 cells/cm^2 were premixed in EBM-2/5% FBS before plating.

In experiments assessing the role of various factors on EC-ASC interactions, cocultures were incubated for 6 days in the EBM-2/5% FBS medium supplemented with (1) neutralizing IgGs to VEGF (2 μg/mL; RnD Systems), or HGF (2 μg/mL; RnD Systems), or corresponding control mouse and goat IgGs (RnD Systems); (2) 10 μM GM6001 (Millipore), an inhibitor of matrix metalloproteinase (MMP) activity with a wide range of activity; (3) 50 μM AG1296 (Alexis), an inhibitor of platelet-derived growth factor (PDGF) receptor β activity; and (4) dimethyl sulfoxide (DMSO), which was used to dilute GM6001 and AG1296, as a negative control. Test cultures were exposed to the varying medium conditions for 6 days.

To separate paracrine from contact-dependent effects of ECs and ASCs on each other, cocultured cells were studied in several additional designs. In the first design, ECs (60×10^3/cm^2) were plated on the lower surface of 24-well Transwell plates, and ASCs (60×10^3/cm^2) were plated in Transwell 8-μm-pore inserts. After adherence of ASCs and ECs to the designated surfaces, inserts were moved into the wells containing ECs. Cocultures were cultivated under EBM-2/5% FBS for 6 days without medium change. A complementary design was identical except that ASCs were plated in the lower chamber, while ECs were plated into inserts. Finally, to specifically evaluate the paracrine effects of ASCs, a mixture of NHDFs and ECs was coplated in the lower chamber, whereas ASCs were plated on the Transwell insert.

Coculture of ECs on ASCs, NHDFs, and SMC monolayers

ASCs, NHDFs, CaSMCs, or AoSMCs were plated at a density of 60×10^3 cells/cm^2 in the EBM-2/5% FBS medium, 3 h before overlaying them with 5×10^3 cells/cm^2 of CBD-ECs as previously described. The mixed cultures were incubated for 6 days with a routine medium change at day 3. In experiments evaluating the effect of the ASC-conditioned medium (ASC-CM) or added growth factors on vascular network formation (VNF), cells were cultured in the EBM-2/5% FBS medium that was either premixed with ASC-CM at a 1:1 ratio or supplemented with VEGF (10 ng/mL) or HGF (10 ng/mL) as single-growth-factor controls.

In experiments evaluating the specific role of ASCs in VNF, nonlabeled ASCs were premixed with NHDFs at ratios of 1:4, 1:9, or 1:19 (ASC:NHDF), or DiI-labeled ASCs were premixed with NHDFs at a ratio of 1:11 (ASC:NHDF). These cell mixtures were plated on cell culture plastic at densities of 60×10^3 cells/cm^2. Three hours later CBD-ECs were seeded on top of the ASC-NHDF monolayers and incubated in EBM-2/5% FBS for 6 days.

Conditioned medium generation

To generate the ASC- or CBD-EC-conditioned medium, cells of each type were grown to confluence in EGM-2mv in T75 flasks, followed by medium replacement with EBM-2/5% FBS. After 1 day, 10 mL fresh EBM-2/5% FBS medium was applied on cell monolayers for 72 h of conditioning. Later ASC-CM and EC-CM were collected, and centrifuged at 300 *g* for 5 min, and supernatants were frozen. Cell number at the time of medium collection was determined using hemocytometer.

Cell suspension analysis by flow cytometry

At the experimental endpoints, cocultures of ASCs with CBD-ECs were harvested, cell numbers were determined using hemocytometer, and cell suspensions were simultaneously incubated for 20 min on ice with CD140b-PE (ASC marker) and CD31-APC (EC markers) IgG (BD). Cells were analyzed for the ASC and EC ratios in coculture and for the intensity of CD31 expression (geometric mean). In a separate set of experiments, cells harvested from ASC monocultures or EC-ASC cocultures wells were simultaneously incubated with Biotinylated Ulex-Lectin (Vector Labs) and anti-NG2 IgGs (Millipore) or with corresponding isotype control mouse IgG, followed by incubation with Streptavidin Alexa 594 and goat anti-mouse APC-labeled IgGs. Flow cytometry was performed using a Calibur flow cytometer and Cell QuestPro software (BD).

Immunohistochemical culture evaluations

Before incubation with antibodies, mono- and cocultures were fixed in methanol at −20°C for 5 min. To evaluate VNF, cocultures were probed with rabbit or mouse anti-CD31 (both 1:50) IgGs, followed by incubation with chicken anti-mouse Alexa 488 IgGs or donkey anti-rabbit Alexa 488 IgGs. For dual stainings, next combinations of antibodies were used—for CD31-laminin and CD31-fibronectin: mouse anti-CD31 and rabbit anti-laminin (1:50) or rabbit anti-fibronectin (1:400); for CD31-α-smooth muscle actin (αSMA), CD31-collagen IV, and CD31-perlecan I: rabbit anti-CD31 IgGs and mouse anti-αSMA IgGs (1:200), or mouse anti-collagen IV (1:25), or rat anti-perlecan (1:50); for Lectin-Caspase 3 or Lectin-Ki67: Biotinyated Ulex lectin (1:600) and rabbit anti-Caspase-3 (1:400) or rabbit anti-Ki67 (1:200). To detect mouse or rat IgGs, cultures were probed with biotinylated horse anti-mouse IgG or rabbit anti-rat IgG (1:250, Vector), followed by incubation with Streptavidin Alexa 594. To detect rabbit IgGs, cultures were probed with donkey anti-rabbit IgG Alexa 488, to detect Biotynilated Ulex lectin—with Streptavidin Alexa 594. Antibodies against CD31, laminin, collagen IV, perlecan, fibronectin, Ki67, and desmin were purchased from LabVision; αSMA and fibronectin IgGs from Sigma; biotinylated IgGs and Ulex Lectin from Vector Labs; caspase-3 from Promega; and all fluorescently labeled IgGs from Invitrogen (dilution 1:200). As a control for specific staining, a separate set of cultures was incubated with mouse, rat, or rabbit isotype control IgGs. Cultures were incubated with antigen-specific or isotype control IgGs for 1 h and with the secondary IgGs for 30 min. The nuclei were counterstained with DAPI.

SDS-PAGE and immunoblot analysis

Mono- and cocultures were harvested with RIPA lysis buffer at different time points and equal amounts of protein were fractionated by 10% (wt/vol) polyacrylamide-resolving gels. After transfer to nitrocellulose membranes, nonspecific protein-binding membranes were blocked with 5% nonfat skim milk/phosphate-buffered saline, incubated with αSMA (1:400; Sigma), fibronectin (1:600; Sigma), or glyceraldehyde 3-phophate dehydrogenase (1:5000; Abcam) IgGs, washed with 0.05% Tween-20/phosphate-buffered saline, incubated with horseradish-peroxidase-conjugated goat anti-mouse or goat anti-rabbit polyclonal IgG (1:10000; Pierce), and washed again. All incubation steps were performed for 1 h at room temperature and wash steps repeated three times with 10 min intervals. Immunoreactive complexes were identified by enhanced chemiluminescence.

Computational and statistical analysis

Fluorescently stained cultures were analyzed using a Nikon TE2000 microscope. Digital images were acquired using a 4× objective (5 pictures/cm^2, 20% of the well surface). Images of vascular networks were processed by MetaMorph software using Angiogenesis Tube Assay algorithm (Molecular Devices).

Quantitative data are expressed as mean ± SEM. Groups were compared by an unpaired *t*-test. Each experiment represents at least $n = 6$. Statistical analysis was performed using Prism 4 (Graphpad).

Results

ASCs stimulate EC cord network formation

To evaluate the potential of ASCs to stimulate and support EC VNF, CBD-ECs were cultured on preformed ASC monolayers. Preliminary experiments (not shown) showed that 60,000/cm^2 of ASCs were sufficient to establish a dense ASC monolayer; plating ASCs at a lower density resulted in partial cell culture plastic coverage and also led to a significantly lower degree of subsequent cord structure formation.

This established standard ASC density was used throughout the study for consistency. Microscopic examination of the wells between days 3 and 6 revealed morphogenesis of the cell monolayers into three-dimensional, cord-like structures in the EC-ASC cocultures (Fig. 1A). At the same time, these structures were present neither in ASC monoculture wells (Fig. 1A) nor in EC monocultures cultivated in the basal medium (Fig. 1A) or exposed to a medium conditioned by ASCs for 72 h (Supplemental Fig. S1, available online at www.liebertonline.com/ten). Moreover, cocultivation of ECs and ASCs in the same well but separated with 8-μm-pore membrane (transwell) also did not lead to cord formation (Supplemental Fig. S1). Staining the cultures with fluorescently labeled antibodies against CD31 revealed that the observed structures were represented by ECs that organized into cords (Fig. 1B). Further, all ECs persisting in the wells incorporated into the cords. Analysis of the plating density of ECs on ASC monolayers versus steady-state network parameters (total tube length, TL; number of branches, B) confirms a specific relationship (Fig. 1C) expressed as

$TL = 14x/(x + 6946)$, and $B = 28x/(x + 9340)$, where x stands for EC plating density (cells/cm^2)

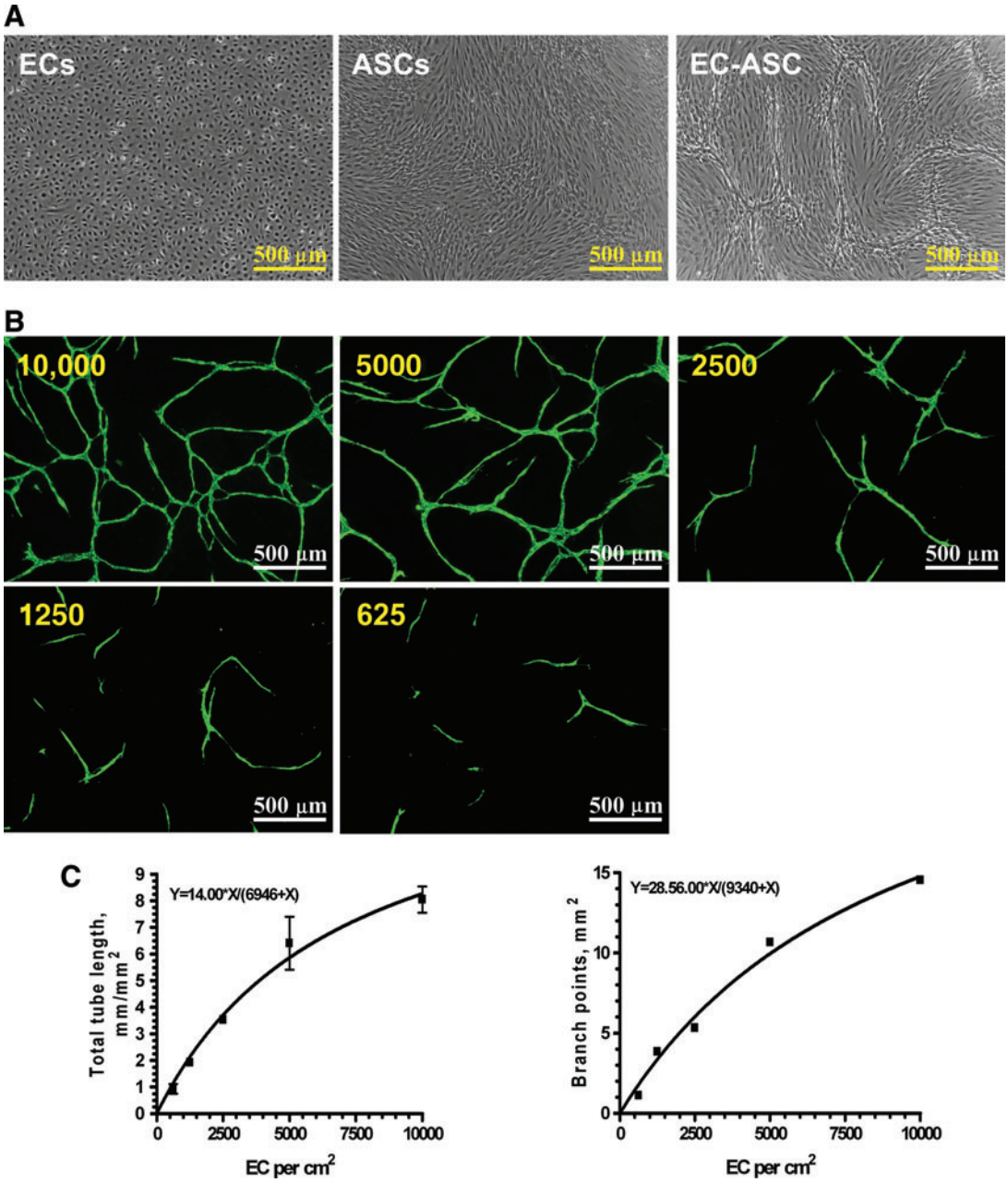

FIG. 1. (**A**) Representative images of cord-blood-derived (CBD) endothelial cell (EC) and adipose stromal cell (ASC) monocultures or their coculture at day 6 postplating. (**B**) Representative fluorescent images of EC-ASC cocultures. CBD-ECs in a range of densities (625–10,000 cells/cm^2) were plated on top of ASC monolayer and cultured for 6 days. EC-formed cord structures were revealed by probing cocultures for CD31 antigen and sequential incubation with Alexa 488–labeled secondary IgGs. (**C**) Quantitative analysis of the correlation between plated EC density (X, cells/cm^2) and vascular network formation (VNF): total tube length and number of branch points ($n = 7$). Color images available online at www.liebertonline.com/ten.

To evaluate vascular network stability, the cocultures were incubated 8, 14, and 21 days postplating, followed by examination (Fig. 2A). Coculturing of ECs and ASCs for 2 weeks resulted in a decrease in total tube length by 18% compared to day 8. The trend was independent from EC plating density. At the same time, further incubation to day 21 was not associated with vascular network degradation.

To determine if the EC VNF on ASC monolayer is an intrinsic behavior of ECs and not specific to CBD-ECs, parallel experiments with immunofluorescent analyses were performed on cocultures of ASCs with ECs isolated from adipose tissue, human umbilical vein EC, and human microvascular EC. Probing cocultures for CD31 antigen revealed that each type of ECs was able to organize into vascular networks when cultured on ASC monolayers (Supplemental Fig. S2, available online at www.liebertonline.com/ten).

Effect of serial versus simultaneous ECs and ASCs plating on VNF

To evaluate whether morphogenesis of ECs to form vascular networks required preplating of ASCs as a feeder layer, experiments were conducted in which ECs and ASCs were also mixed at a 1:12 ratio (EC:ASC, same ratio as in layer plating method) and plated simultaneously. Analysis of VNF revealed that preformation of a stromal monolayer was not mandatory (Fig. 2B); in fact, after premixing, ECs assembled into networks with higher efficiency (total tube lengths of $6.24 \pm 0.31\,mm/mm^2$) than VNF in case of sequential method of cell plating, yielding total tube lengths of $4.87 \pm 0.47\,mm/mm^2$ ($p \leq 0.01$).

Persistence of the cells in ASC-EC coculture

Analysis of the cell persistence in cocultures revealed a slight decrease in cell number during the first 3 days of EC-ASC cultivation, $19.1\% \pm 10.3\%$ for ECs and $10.2\% \pm 10.3\%$ for ASCs, whereas no significant change in cell numbers was observed between days 3 and 6 (Fig. 2C, D). To evaluate the EC and ASC fate during cultivation, cultures were probed for Ki67 (marker of proliferating cells) or active caspase-3 (marker of apoptosis) at day 3 postplating. Analysis of the wells revealed that while in the EC monocultures some cells were positive for Ki67, there was a very low number (if any) of Ki67-positive cells detected in ASC monocultures and EC-ASC cocultures (Supplemental Fig. S3, available online

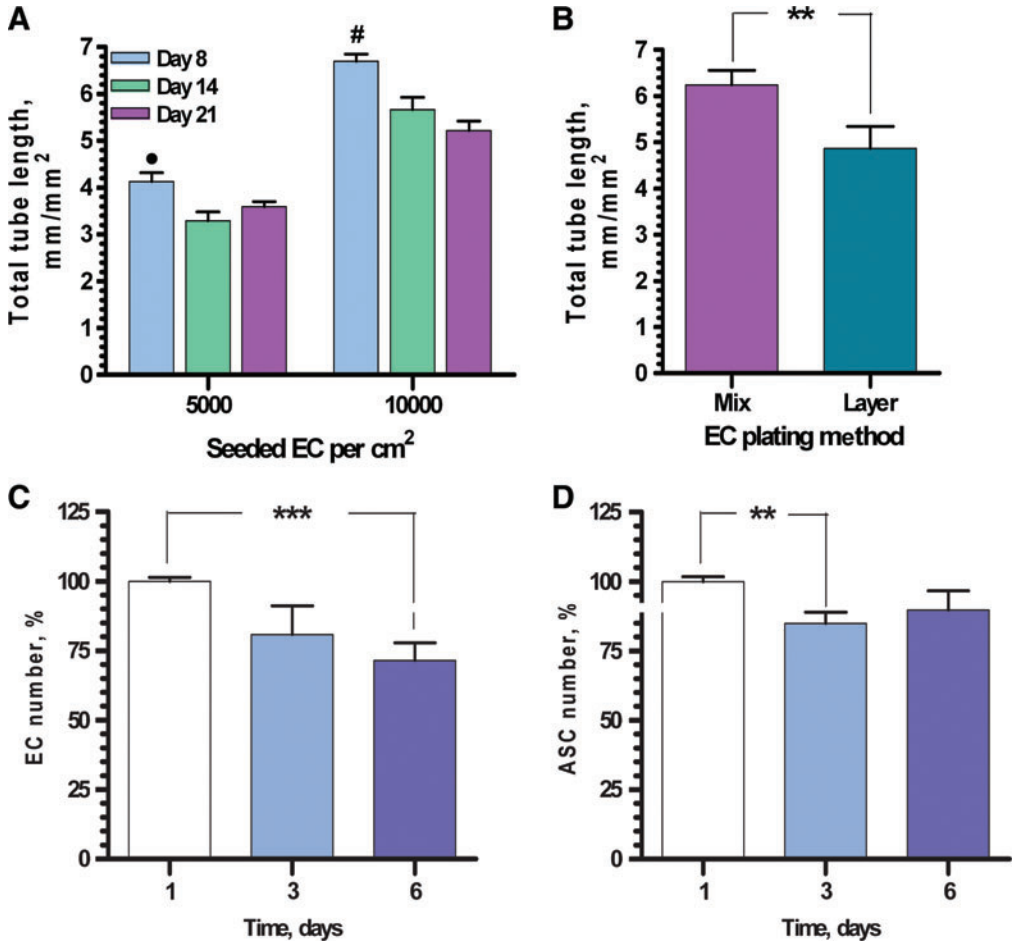

FIG. 2. (**A**) Quantitative analysis of the vascular network stability during first 3 weeks of cultivation (total tube length, $n = 12$). •, $^{\#}p \leq 0.05$ between day 1 and days 14 and 21 for ECs seeded at the densities 5000 and 10000 cells per cm^2 correspondingly. (**B**) Comparative quantitative analysis of VNF by ECs plated in mixture with ASCs (simultaneous plating, "Mix") or after ASC monolayer formation (3 h post-ASC plating, "Layer") ($n = 9$, $^{**}p \leq 0.01$). (**C, D**) Analysis of ECs (**C**, CD31 + cells) and ASCs (**D**, CD140 + cells) persistence in cocultures during 6-day period ($n = 12$, $^{**}p \leq 0.01$, $^{***}p \leq 0.001$). Color images available online at www.liebertonline.com/ten.

at www.liebertonline.com/ten). Similar to that, caspase-3-positive cells were detected in EC monocultures, but not in ASC monocultures or EC-ASC cocultures (Supplemental Fig. S4, available online at www.liebertonline.com/ten).

Migration and upregulation of αSMA expression by ASCs in EC-ASC coculture system

Formation of vascular networks by ECs was accompanied by ASC migration and accumulation in direct proximity to EC cords, producing an elevated density of cells near the cords (based on DAPI staining) and reduction in density between cords (Fig. 3A, middle right). Culture of ASCs alone in the EBM-2/5% FBS medium resulted in relatively low and diffused expression of αSMA with a nonfilamentous diffuse distribution (Fig. 3A top left, B). However, coculture of ASCs with ECs resulted in significant increase in αSMA expression (Fig. 3B), and its organization into fibers, selectively in those ASCs that were in direct contact or in proximity with ECs (Fig. 3A, top right and middle left). To evaluate if direct contact of ASCs with ECs is crucial for upregulation of αSMA expression or whether the EC-conditioned medium can provide a similar effect, ASC monocultures were exposed to the EC-conditioned medium for 6 days. Staining of these monocultures for αSMA revealed no upregulation of antigen expression (Fig. 3A, bottom left). Similarly, no

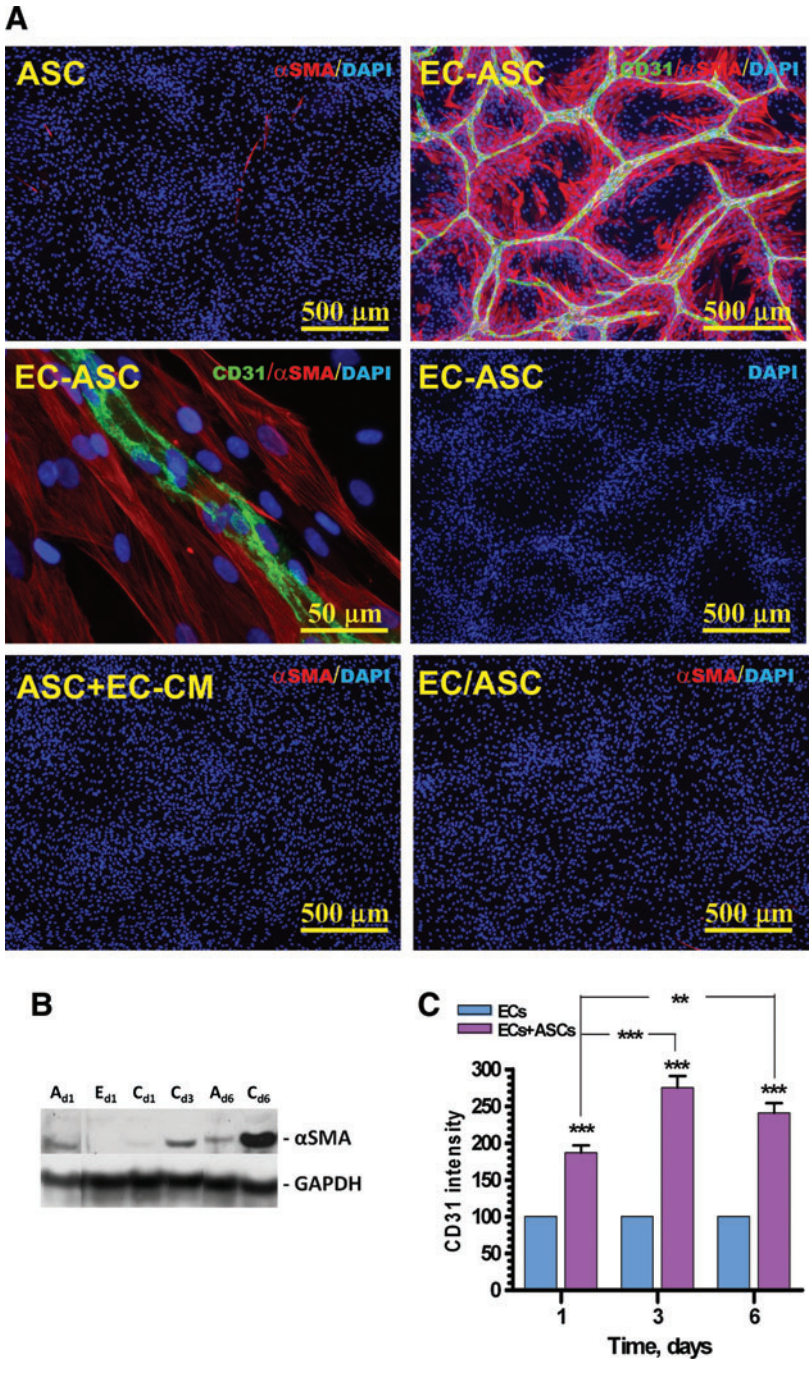

FIG. 3. (**A**) Representative images of ASC monocultures (ASC), EC-ASC coculture (EC-ASC), ASC cultures in the medium conditioned by ECs (ASC + EC-conditioned medium [CM]), and ASCs cocultured with ECs without physical contact (EC/ASC) that were probed for α-smooth muscle actin (αSMA) (red) and CD31 (green) at day 6 postplating. Nuclei were revealed by DAPI staining (blue). (**B**) Analysis of α-smooth muscle actin protein expression in ASC ("A") and EC ("E") monocultures and EC-ASC cocultures ("C") at days 1, 3, and 6 by Western blot. Expression of glyceraldehyde 3-phophate dehydrogenase protein was used as a control for the protein loading. (**C**) Analysis of CD31 antigen surface presentation on ECs cultured alone or together with ASCs for up to 6 days ($n = 10$) (**$p \leq 0.01$, ***$p \leq 0.001$). Color images available online at www.liebertonline.com/ten.

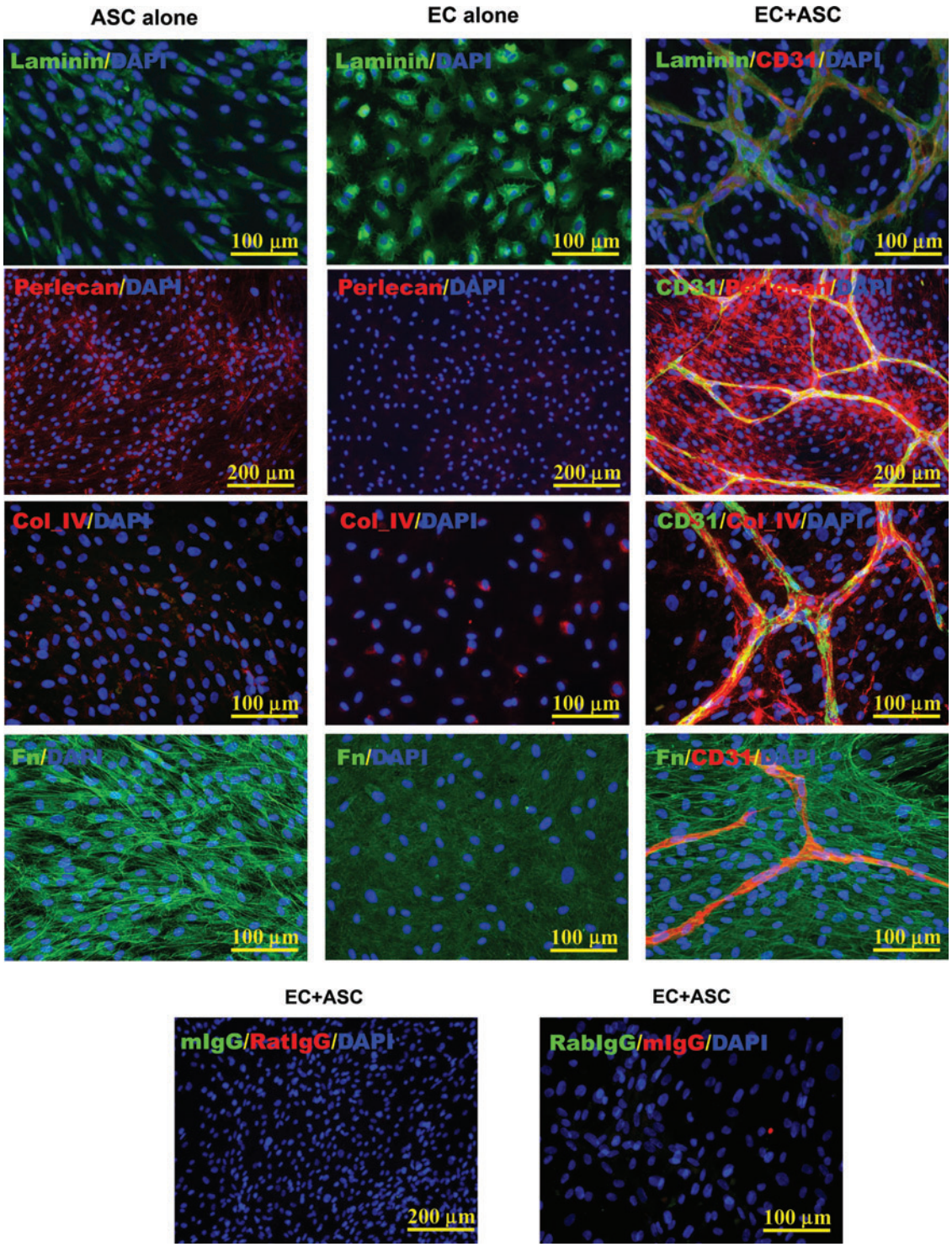

FIG. 4. Representative images of ASC and EC monocultures and EC-ASC cocultures probed for laminin, perlecan, collagen IV (Col_IV), and fibronectin (Fn) (all) and CD31 antigen (only cocultures). As a control, parallel EC-ASC cocultures were probed with isotype control IgG. Nuclei were revealed by DAPI staining. Color images available online at www.liebertonline.com/ten.

upregulation of αSMA expression was detected when ASCs were cultivated with ECs in the same well but physically separated from them by 8-μm-pore membranes in Transwell dishes (Fig. 3A, bottom right). Analysis of expression of other markers typical for pericytes, NG2 and desmin, revealed that even though ASCs express both of these antigens without any additional stimuli (NG2 not shown; desmin, see Supplemental Fig. S5, available online at www.liebertonline.com/ten), exposure of ASCs to ECs did not significantly affect the level of their expression.

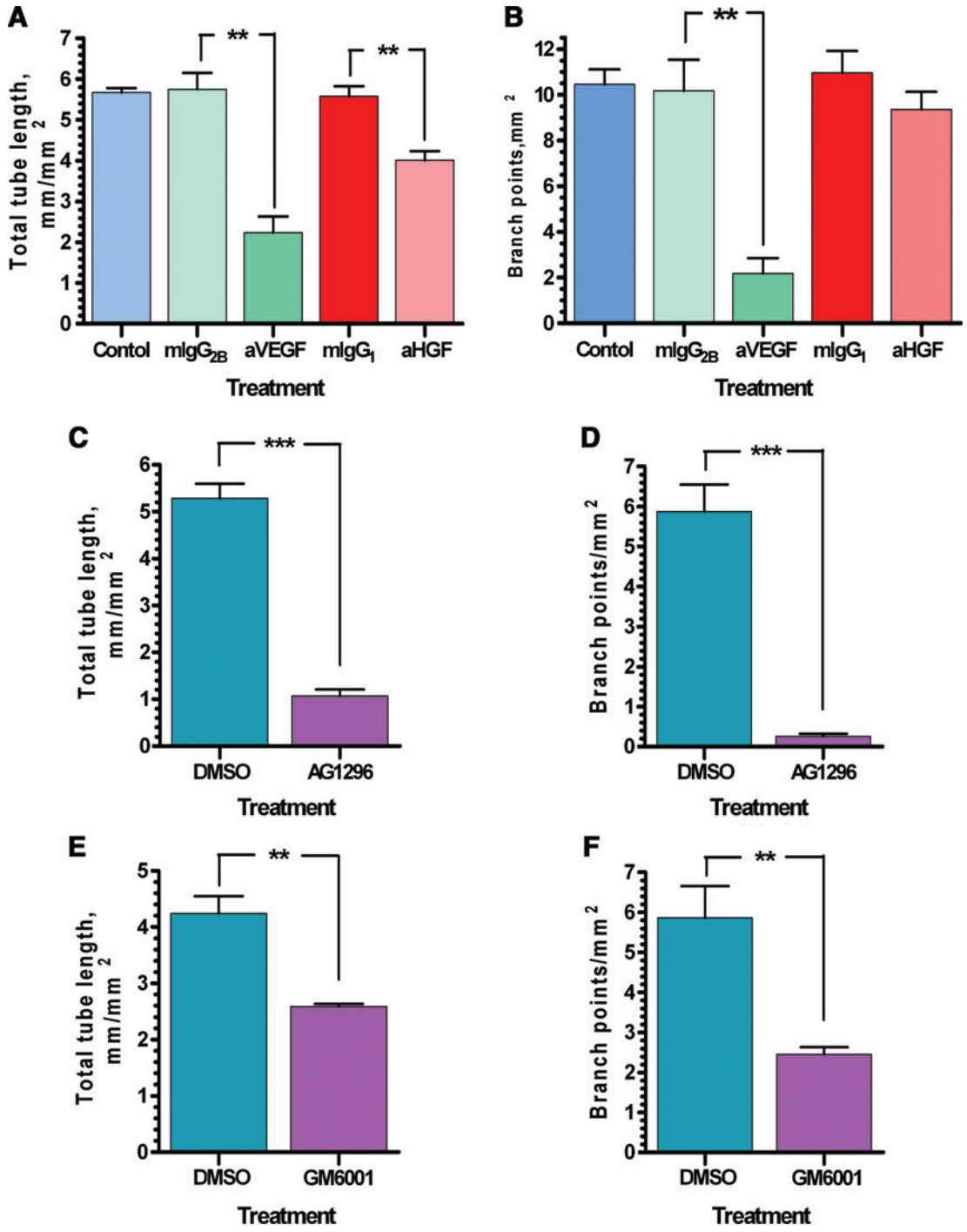

FIG. 5. Quantitative analysis of the VNF (density of total tube length and branch points) by EC-ASC cocultures exposed to (**A, B**) EBM-2/5% fetal bovine serum (FBS) medium alone or supplemented with anti-vascular endothelial growth factor (a-VEGF), anti-hepatocyte growth factor (a-HGF) IgG, or their isotype control mouse (mIgGs) for 6 days ($n = 3$); (**C, D**) EBM-2/5% FBS medium supplemented with dimethyl sulfoxide (DMSO) or AG1296 for 6 days ($n = 6$); (**E, F**) EBM-2/5% FBS medium supplemented with dimethyl sulfoxide or GM6001 for 6 days ($n = 4$) (**$p \leq 0.01$, ***$p \leq 0.001$). Color images available online at www.liebertonline.com/ten.

At the same time, coculturing ECs with ASCs led to an increase in extracellular presentation of EC antigen CD31/PECAM by up to $275\% \pm 16\%$ at day 3 in comparison with EC cultured alone ($p < 0.001$) (Fig. 3C). There was no further change in the level of CD31 expression between days 3 and 6 (length of experiment).

ECM protein production by ASCs in EC-ASC coculture system

As shown in Figure 4, expression of laminin was detected in both ASC and EC monocultures as well as in coculture settings. Double staining in coculture with anti-CD31 and

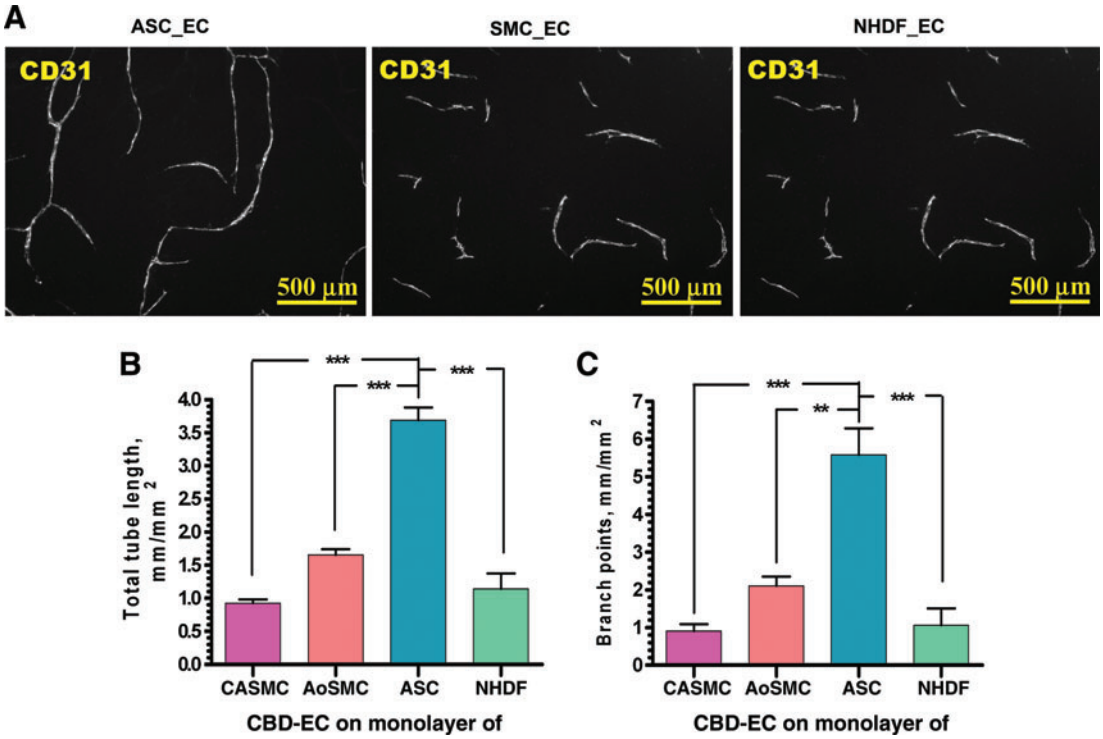

FIG. 6. (**A**) Representative images of vascular cord structures (CD31 staining) formed by CBD-ECs cultured on ASC, coronary artery smooth muscle cell (CaSMC), or normal human dermal fibroblast (NHDF) monolayers revealed at day 6 postplating. (**B, C**) Quantitative analysis of the vascular tube (**B**) and branch point (**C**) density in the vascular networks formed by CBD-ECs cultured on CaSMC, aortic (Ao)SMC, ASC, or NHDF monolayers for 6 days ($n=7$ for ASCs and CaSMCs; $n=6$ for NHDFs; $n=4$ for aortic SMCs, $^{**}p\leq 0.01$, $^{***}p\leq 0.001$). Color images available online at www.liebertonline.com/ten.

laminin IgGs revealed that although laminin was present throughout the cultures, the pattern of its highest level of accumulation mirrored the geometry of EC cord structures. Expression of collagen IV was not detected in ASC monoculture, but was present in a low level in EC monoculture. At the same time, expression of this protein by ECs was significantly increased in cocultures, and the pattern of its accumulation was restricted to the surfaces of the EC-cord structures. A significant level of fibronectin expression was observed in ASC monocultures and low level in EC cultured alone (Fig. 4 and Supplemental Fig. S6, available online at www.liebertonline.com/ten). At the same time, exposure of ASCs to ECs led to significant increase in this protein expression (Supplemental Fig. S6) and its extracellular accumulation in fibrillar form. Finally, expression of perlecan I was detected in a low level in ASC monoculture, but not in EC monoculture, while in coculture the perlecan I expression was also significantly increased, displaying a clear pattern of distribution: with highest density of its accumulation in proximity to the EC-cord structures.

Effect of neutralizing IgGs and chemicals on VNF

To evaluate the importance of selected angiogenic factors for VNF, cocultures were exposed to the basal medium containing neutralizing IgGs to two factors secreted in significant quantities by ASCs: VEGF and HGF. The presence of anti-VEGF IgG in the medium led to decrease in total tube lengths from $5.75\pm0.4\,mm/mm^2$ (control, in the presence of mouse IgG_{2b}) to $2.23\pm0.4\,mm/mm^2$ ($p\leq 0.01$; Fig. 5A, B). Network branching decreased to a proportionally greater degree: from 10.18 ± 1.36 branches/mm^2 for $mIgG_{2b}$ to 2.18 ± 0.68 branches/mm^2 for anti-VEGF IgGs ($p\leq 0.01$). Interestingly, while anti-HGF treatment inhibited total tube length in the networks from $5.58\pm0.24\,mm/mm^2$ for control (in the presence of $mIgG_1$) to $4.01\pm0.22\,mm/mm^2$ for anti-HGF IgGs ($p\leq 0.01$), it had proportionally less effect on the degree of network branching: 9.36 ± 0.78 branches/mm^2 with anti-HGF IgGs versus 10.96 ± 0.97 branches/mm^2 with $mIgG_1$.

The role of PDGF-BB, which is secreted in significant amounts by ECs (not shown), in VNF was evaluated by exposing cells to the chemical inhibitor of PDGF receptor β—AG1296 (50 μM). Inhibition of PDGF receptor β led to marked reduction of VNF (Fig. 5C, D) based on total tube length: from $5.29\pm0.31\,mm/mm^2$ for DMSO to $1.07\pm0.14\,mm/mm^2$ for AD1296 ($p\leq 0.001$) and degree of network branching: from 5.88 ± 0.67 branches/mm^2 for DMSO to 0.26 ± 0.06 branches/mm^2 for AG1296 ($p\leq 0.001$).

The role of MMPs in VNF was tested by exposing cocultures to the medium containing 10 μM of GM6001, an inhibitor of MMP-1, 2, 3, 8, and 9, or to DMSO as a control (Fig. 5E, F). On the basis of total tube length, $4.24\pm0.31\,mm/mm^2$ for control versus $2.59\pm0.05\,mm/mm^2$ for GM6001 ($p\leq 0.01$), and the degree of network branching, 5.86 ± 0.79 per mm^2 for control versus 2.45 ± 0.17 per mm^2 for GM6001 ($p\leq 0.01$), we conclude that MMPs also played an essential role in VNF with respect to both overall assembly and branch formation.

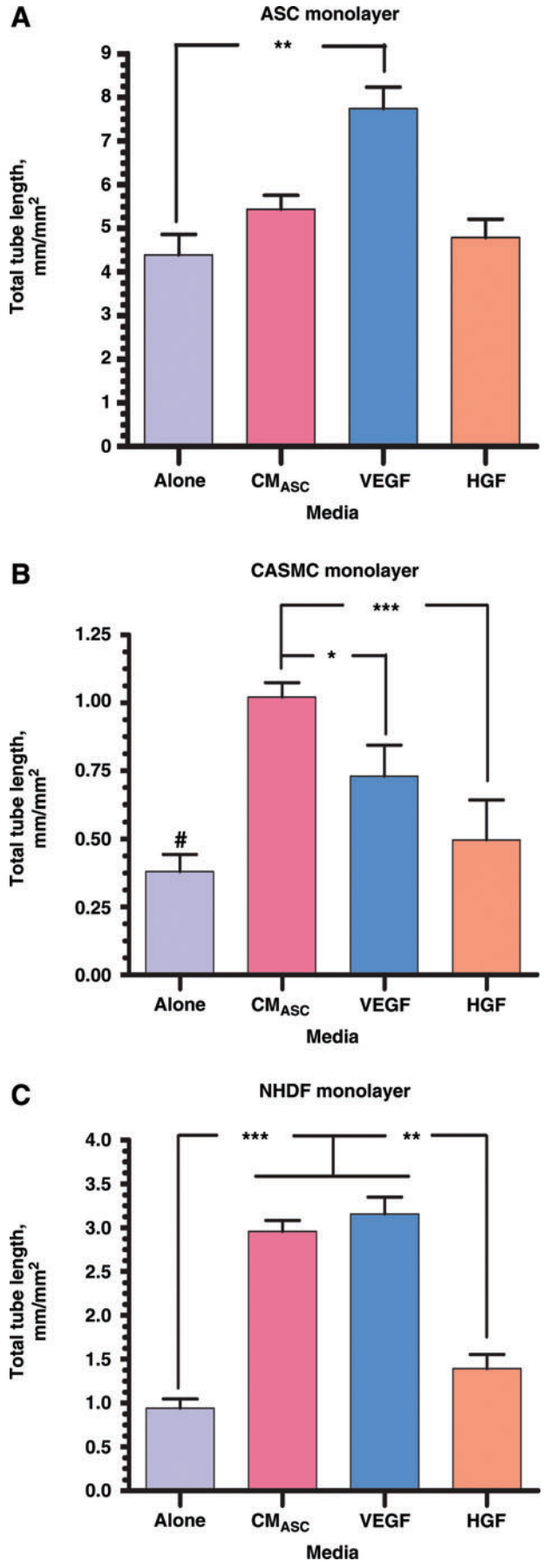

Comparative analysis ASCs, SMCs, and fibroblasts with potential to support VNF

To evaluate whether the ability to stimulate VNF by ECs is a unique characteristic of ASCs or if other cell types possess similar activity, we performed direct comparative analysis of VNF by ECs on monolayers of ASCs, SMCs, and dermal fibroblasts plated in parallel (Fig. 6). Anti-CD31 staining revealed that ASCs promote VNF much more strongly than the other tested cell types based on total tube length ($3.69 \pm 0.19\,mm/mm^2$) and network branching ($5.58 \pm 0.7\,mm^{-2}$). ECs cultured on SMCs and fibroblasts established networks with significantly lower total tube length: $0.92 \pm 0.06\,mm/mm^2$ for CaSMCs, $1.65 \pm 0.08\,mm/mm^2$ for AoSMCs, and $1.14 \pm 0.23\,mm/mm^2$ for fibroblasts ($p \leq 0.001$ ASC vs. all other cell types) and branching: 0.91 ± 0.18 per mm^2 for CASMCs, 2.11 ± 0.24 per mm^2 for AoSMCs, and 1.06 ± 0.45 per mm^2 for fibroblasts ($p \leq 0.001$ ASCs vs. CaSMCs and fibroblasts, $p \leq 0.01$ ASCs vs. AoSMCs).

To test the overall role of the soluble factors secreted by ASCs on VNF, cocultures of ECs with ASCs, SMCs, and fibroblasts were exposed for 6 days either to ASC-CM or to specific factors secreted by ASCs, VEGF, and HGF[22,23] (Fig. 7). In EC-ASC cocultures, only VEGF supplementation significantly augmented network development, increasing total tube length by 76%. EC cultured on CaSMC or fibroblast monolayers in the presence of ASC-CM resulted in increased total tube lengths by 3.12 and 3.15 times, respectively, by comparison with coculture in the control medium (EC-CaSMC/Control: $0.37 \pm 0.13\,mm/mm^2$; EC-CaSMC/ASC-CM: $1.12 \pm 0.08\,mm/mm^2$; EC-fibroblast/Control: $0.94 \pm 0.11\,mm/mm^2$; EC-fibroblast/ASC-CM: $2.96 \pm 0.13\,mm/mm^2$). A similar trend was observed when cocultures were exposed to VEGF (EC-CaSMC/VEGF: $0.9 \pm 0.18\,mm/mm^2$; EC-fibroblast/VEGF: $3.16 \pm 0.19\,mm/mm^2$) and HGF (EC-CaSMC/HGF: $0.74 \pm 0.21\,mm/mm^2$; EC-fibroblast/HGF: $1.4 \pm 0.16\,mm/mm^2$. While supplementation of EC – CaSMC and EC-fibroblast cocultures with ASC-CM, VEGF, or HGF significantly stimulated VNF, none of these treatments were able to reach the degree of VNF demonstrated by direct contact of ECs with ASCs in the control medium.

To evaluate whether the stimulation of VNF was dependent on the distinctive medium used for growing cells, complementing ECs, ASCs, and fibroblasts were expanded for two passages either in their typical medium (ASCs with EGM-2mv and fibroblasts with FGM-2) or in the medium normally used for expanding the alternative cell type (ASCs in FGM-2 and fibroblasts in EGM-2mv). The ASCs and fibroblasts were subsequently cocultured with CBD-ECs.

FIG. 7. Quantitative analysis of the vascular tube density establish by ECs cultured on ASC (**A**), CaSMC (**B**), and NHDF (**C**) monolayers for 6 days in the basal medium alone or supplemented with one of the next: ASC-conditioned medium (CM_{ASC}), 10 ng/mL VEGF, or 10 ng/mL HGF ($n \geq 3$ for Alone, VEGF, and HGF and $n \geq 9$ for CM_{ASC} ($^{*}p \leq 0.05$, $^{**}p \leq 0.01$, $^{***}p \leq 0.001$). $^{\#}p \leq 0.001$ between "Alone" and "CM_{ASC}" and $p \leq 0.05$ between "Alone" and "VEGF" in CASMC monolayer setting. $''p \leq 0.001$ between "CM_{ASC}" and "Alone", "VEGF" and "Alone" and $p \leq 0.01$ between "CM_{ASC}" and "HGF", "VEGF" and "HGF" in NHDF monolayer setting. Color images available online at www.liebertonline.com/ten.

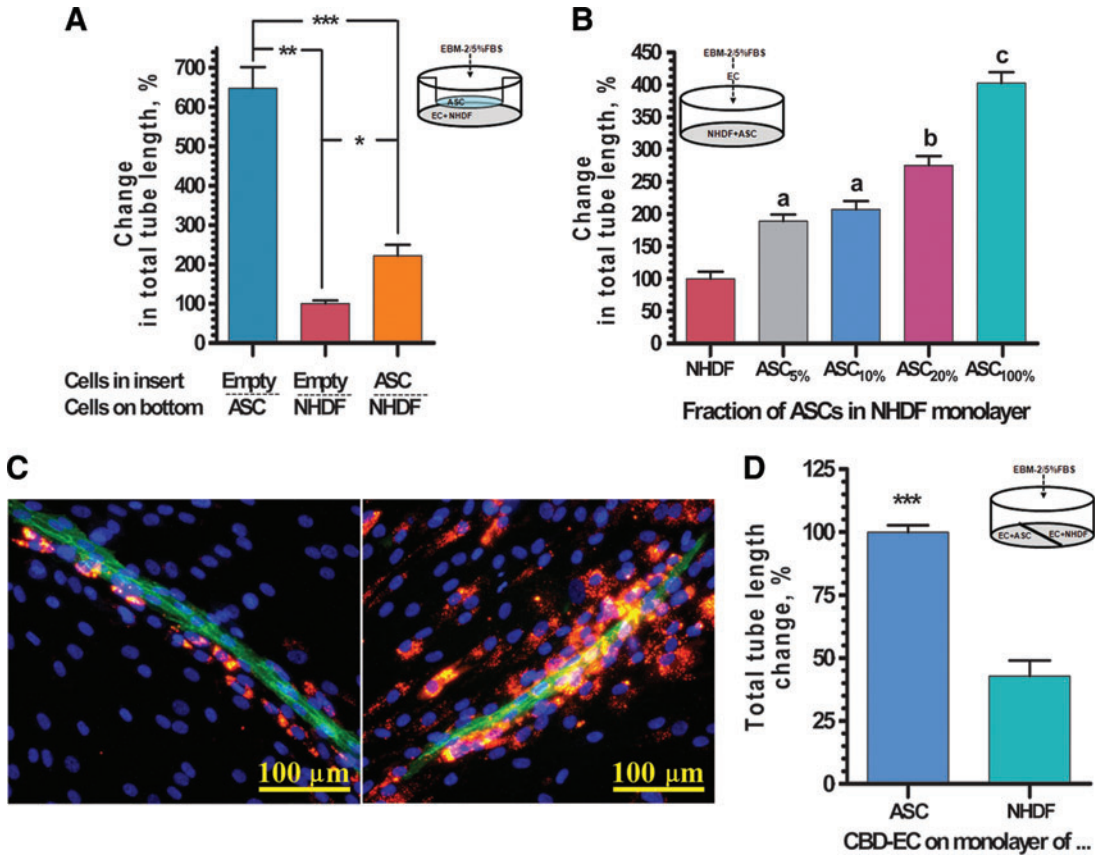

FIG. 8. (**A**) Quantitative analysis of VNF by ECs cultured in Transwells on ASC or NHDF monolayer in the presence of empty inserts or on NHDF monolayer in the presence of insert confluently seeded with ASCs ($^{*}p \leq 0.05$, $^{**}p \leq 0.01$, $^{***}p \leq 0.001$). (**B**) Quantitative analysis of VNF by ECs added onto either a preformed ASC monolayer (right bar) or on NHDF monolayers supplemented with 0%–20% of ASCs ($n = 9$; $^{a}p \leq 0.01$ between NHDF and $ASC_{5\%}$ and between NHDF and $ASC_{10\%}$; $^{b}p \leq 0.01$ between $ASC_{20\%}$ and NHDF-$ASC_{10\%}$; $^{c}p \leq 0.01$ between $ASC_{100\%}$ and NHDF-$ASC_{20\%}$). (**C**) Two representative immunofluorescent images of vascular cord structures formed by ECs (revealed by CD31 staining, green) on monolayer composed of NHDFs (nonlabeled) and 8% of DiI-labeled ASCs (red). Nuclei revealed by DAPI staining (blue). (**D**) Comparative analysis of VNF by ECs in EC-NHDF and EC-ASC setting when two cocultures were able to share the culture medium, but were physically separated ($^{**}p \leq 0.01$). Color images available online at www.liebertonline.com/ten.

Analysis of the networks at day 6 revealed that the potential of the ASCs to stimulate EC VNF was not affected by the medium used for ASC expansion (Supplemental Fig. S7, available online at www.liebertonline.com/ten). Fibroblasts expanded in the EGM-2mv medium had slightly better effects on VNF than fibroblasts expanded in FGM-2, but this effect was approximately threefold lower than the network development observed with ASCs expanded in either the FGM-2 or the EGM-2mv medium.

In a separate set of experiments we evaluated whether factors secreted by ASCs in real time during the course of VNF would have similar effect on VNF as a medium preconditioned by ASC monoculture during a 72-h period (as shown in Fig. 7). In these studies (Fig. 8A) ECs cultured on top of ASCs were able to establish a 6.5-fold denser vascular network than ECs cultured on an NHDF monolayer ($647\% \pm 54\%$ and $100\% \pm 8\%$ correspondingly), while the addition of Transwell inserts confluently seeded with ASCs (selective evaluation of paracrine ASC activity) led to an increase in VNF on NHDFs by 2.2 times ($222\% \pm 27\%$).

To evaluate whether the physical presence of ASCs would also stimulate VNF in an EC-fibroblast system, ASCs were premixed with NHDFs in ratios from 1:19 to 1:4 (ASC:NHDF) before plating, followed by overlay with ECs. Comparative analysis of the networks formed by ASCs and fibroblasts alone or in their mixtures demonstrated that ASCs presented in the fibroblast monolayer were able to dose dependently increase total tube length of the vascular network: 189.1 ± 10.3, 207.3 ± 13.2, 275.3 ± 14.3, and 402.6 ± 17.0 for the monolayers containing 5%, 10%, 20%, and 100% of ASCs, respectively, compared to the ones that were formed by NHDFs alone (Fig. 8B).

To evaluate if this effect was exclusively due to ASC paracrine action (including real-time cross-talk between ASCs and ECs) or whether direct physical interaction between ASCs with ECs also plays an important and distinct role in promoting VNF by ECs, we performed a set of experiments in which EC-NHDF and EC-ASC cocultures were incubated in a single well, thus sharing a common culture medium, yet were spatially separated from each other. This setup allowed free diffusion and distribution of all soluble factors produced by each cell type in the system, but prevented ASCs, fibroblasts, or ECs to migrate between the two compartments of the well. As shown in Figure 8C, even

though in this design, EC-NHDF cocultures were able to take advantage of all soluble factors that were cumulatively produced by ECs and ASCs in EC-ASC cocultures, the level of VND by ECs in direct contact with NHDFs remained 60% lower than that observed for ECs in direct contact with ASCs in the same well (100.0% ± 2.8% and 42.7% ± 6.2% for EC-ASC and EC-NHDF cocultures, respectively). These data specifically suggest that immediate proximity or contact of ECs with ASCs plays a crucial role in ASC-mediated VNF, not achieved by soluble factors alone.

To evaluate the dynamics of ASC interaction with ECs, ASCs were labeled with the fluorescent dye DiI before mixing with fibroblasts and plating (mixing ratio 1:11, ASC:NHDF). Analysis of colocalization of ECs (stained for CD31 antigen) with DiI-labeled ASCs at day 6 revealed that ASCs were localized in proximity to EC cords (Fig. 8D). Additionally, the relative density of labeled ASCs was markedly depleted in areas distant from the EC cords, demonstrating clear tropism of ASCs toward endothelial tubes even in the context of an excess of fibroblasts. This phenomenon helps explain the observation that VNF is associated with increased nuclear density in regions proximate to the EC cord structures (Fig. 3A, middle right).

Discussion

In contrast with the majority of previously described *in vitro* vasculo- and angiogenic coculture models, for example, Matrigel assays,[27] aortic ring assay,[28] and bead/fibrin gel assay,[29] the model presented in this study is free from exogenously added ECM proteins as well as additional cytokines and growth factors (only exposed to the 5% serum). We believe that these features of our model make dissection of the communications (direct physical contact and paracrine crosstalk) between complementary vasculogenic cell types less susceptible to the confounding effects of the exogenous factors provided to the system.

The observations that certain types of adult progenitor cells can be efficiently expanded *in vitro* without losing angiogenic properties has raised the enthusiasm for the development of autologous cardiovascular cell therapies. However, the absence of reliable methods to validate the therapeutic potentials of the isolated/expanded cells before implantation creates uncertainty in predicting the efficacy of these therapies. For example, it is well known that physiological and pathological factors such as age, diabetes, and hyperglycemia[30] significantly decrease the therapeutic potential of the cells. Further, there may be many other undefined subject-specific factors that can significantly compromise therapeutic potential of the cells. Pretesting for cell potency *in vitro* using vasculogenic models, such as the one demonstrated here, before their use in therapy will provide some *a priori* knowledge about the efficacy of a cell treatment. Using well-defined gold-standard ECs and well-defined mural cells, for example, a population of ASCs as described in this report, an assay could be conducted to screen the vasculogenic/angiogenic potential of progenitor cells of each kind before implantation. Moreover, the simplicity of the model setup and its duration (3–6 days), as well as data acquisition followed by potentially automated computer-assisted analysis,[31] renders this model useful for testing different pro- and antiangiogenic compounds.

The present study illuminates the interactions between the endothelial cells and ASCs, which we and others have described as pre-pericytes,[22,32,33] which lead to mature vessel formation.[24] Understanding of these interactions will help elucidate the previously observed vasculogenic/angiogenic effects of ASCs.[22–24,34,35] Defining the mechanisms by which new vessel formation can be augmented may also improve the design of vascular therapies that are based on EC-ASC dual-cell systems.

In the past decade, there have been multiple studies demonstrating that ASCs are able to restore blood flow to ischemic tissues[28,31–33] and support vessel formation by ECs.[24] Despite these observations, the exact mechanisms responsible for these effects are not well defined. The most accepted hypothesis of ASC action is secretion of angiogenic and antiapoptotic factors, which stimulates host tissue preservation and angiogenesis. However, our recent observations have demonstrated that ASCs are localized in the peri-endothelial layer of their native bed—adipose tissue—and after isolation and purification possess or can acquire properties of pericytes in *in vitro*[22] and *in vivo* models,[24] thus suggesting an additional potential function of these cells that may mediate their therapeutic action.

The experiments with neutralizing antibodies to angiogenic factors support our prior *in vivo* observations that VEGF and HGF, factors that are secreted by ASCs in significant amounts, as well as PDGF-BB, of endothelial origin, are essential for EC-ASC VNF. While blocking the activities of VEGF and HGF in the EC-ASC cultures significantly reduce the degree of VNF, the exogenous introduction of these factors to EC-NHDF and EC-SMC cocultures significantly promoted VNF. However, VEGF, HGF, or ASC-CM could not be used to completely replace the effects of ASC presence in cocultures to promote VNF. We accordingly conclude that direct interaction between ECs and ASCs plays a crucial role in efficient VNF.

As we showed previously, the majority of ASCs, whether freshly isolated or expanded (EGM-2mv), exhibit a low level of αSMA antigen expression.[22] We found that ASCs subcutaneously coimplanted in gels with ECs in mice exhibited upregulated expression of αSMA,[24] but the factors responsible for this effect were undefined. The present *in vitro* study revealed that ASCs that were adjacent to ECs specifically displayed induction of αSMA expression and its organization into fibers, suggesting the hypothesis that ECs induce a differentiation program in ASCs including αSMA expression and fibrillogenesis, as well as an increase in fibronectin and perlecan I production (Figs. 3A, B and 4).

The results of this study demonstrate that ASCs exhibit a significantly higher potential to promote VNF in concert with ECs than either SMCs or fibroblasts. Despite the ability of the ASC-conditioned medium or angiogenic factors (VEGF or HGF) to augment VNF on SMCs and fibroblasts (Figs. 7 and 8A), none of these supplements were able to substitute for direct interaction between ECs and ASCs (Fig. 8D). These observations suggest that physical interaction between ECs and ASCs as well as unique features of the ASC secretome that emerge as a result of interaction with ECs are playing crucial roles in VNF. These complementary hypotheses are well supported by our observation that low doses of ASCs (5%–20%) in EC-fibroblast cultures significantly promoted VNF (Fig. 8B), but these effects were not exclusively due to ASC paracrine activity, as it was not able to promote VNF in the EC-NHDF mixture to the same degree as in the EC-ASC

mixture, when these two cocultures were coincubated in one well and were able to share the culture medium (Fig. 8D). The mechanisms of interactions between EC-ASC that lead to VNF and specifically accumulation of ASCs in direct proximity to ECs and stimulation of vasculogenesis are yet unknown and will be the aim of future studies.

It is well known that ECM proteins such as laminin,[36] fibronectin, perlecan-1,[37,38] and collagen IV[39] are integral components of vasculogenesis. This study demonstrated that the VNF was associated with extracellular accumulation of these factors. While the expression of laminin was not substantially increased in coculture, expression of collagen IV by ECs and perlecan-1 and fibronectin by ASCs was upregulated in cocultures, and their highest level of accumulation (for collagen IV and perlecan-1) was specifically in the regions of vascular tube formation. Accordingly, we hypothesize that substantial accumulation of ECM proteins in the areas of ASC and EC colocalization produced favorable conditions (including creating binding sites for integrins and growth factors) for ECs to assemble into neovessels. The hypothesis that ECM proteins play a crucial role in VNF is further supported by observation that blockage of MMPs responsible for ECM protein remodeling as well as growth factor activation led to significant reduction of VNF.

The *in vitro* demonstration that plating ECs and ASCs together induces joint organization into vascular cord structures provides a deeper understanding of our previous observation that mixtures of ECs with ASCs were able to establish multilayered functional vessels in mouse tissue (ear pinnae) even without additional support of exogenously added ECM proteins.[24] These observations also strongly support our primary concept that local injection of ASCs together with ECs can significantly increase blood supply in under-perfused tissues by promoting assembly of ECs into mature stable vessels and establishing connections with the host vasculature.

Taken together, the data acquired in this study permit us to propose a model for a sequence of events leading to initiation, development, and stabilization of vascular structures *in vitro* and ASCs differentiation from progenitors into mature mural cells. ECs' contact with ASCs leads to modulation of cytokine secretion and complementary accumulation of ECM protein produced by ASCs and ECs. These bioactivities of the cells in turn induce EC assembly into cord structures, in parallel with increased expression of PECAM-1 on the EC surface—one of the key signs of initial vessel maturation.[40,41] The formation of cord structures is accompanied by induction of an EC secretory program that in turn stimulates ASCs to migrate and further accumulate in the direct proximity to the EC cords (Fig. 8C), followed by ASCs incorporation into the vessel wall and transforming from αSMA^{dim} into αSMA^{bright} expressing cells, likely enabling initial contractility of the developing vessels. We propose that *in vivo* this sequence of events will lead to multilayered mature vessel formation, which will correlate with gradual downregulation of angiogenic factors and matrix protein production. Each step of this proposed sequence is readily amenable to more extensive analysis in this model, and is consistent with our previous *in vivo* observations demonstrating that subcutaneous implantation of EC-ASC mixture in collagen/fibronectin gels leads to multilayer functional vessel formation with vessel outer layers comprised of αSMA-expressing ASCs.[24]

Conclusion

Using a newly developed *in vitro* model of vasculogenesis that is substantially free of exogenous cytokines and ECM proteins, we have demonstrated for the first time the initial events of interaction between ECs and adipose progenitor cells with characteristics of pre-pericytes. This system enables unique insights into the process of vascular morphogenesis as well as differentiation of readily available progenitors from adipose tissue toward pericytes.

Acknowledgments

This research was supported by NIH R01 HL77688-01 and VA Merit Review grants (to K.L.M.); AHA Postdoctoral award 0727777Z (to D.T.); Cryptic Mason's Medical Research Foundation, and IUPUI VC-CAST Signature Center.

Disclosure Statement

No competing financial interests exist.

Author Contribution

Stephanie Merfeld-Clauss: conception and design, collection and/or assembly of data, and data analysis and interpretation.

Nagesh Gollihalli: Collection and/or assembly of data, and data analysis and interpretation.

Keith L. March: Conception and design, financial support, data analysis and interpretation, and manuscript writing.

Dmitry Traktuev: Conception and design, financial support, collection and/or assembly of data, data analysis and interpretation, manuscript writing, and final approval of manuscript.

References

1. Asahara, T., and Isner, J.M. Endothelial progenitor cells for vascular regeneration. J Hematother Stem Cell Res **11,** 171, 2002.
2. Masuda, H., and Asahara, T. Post-natal endothelial progenitor cells for neovascularization in tissue regeneration. Cardiovasc Res **58,** 390, 2003.
3. Kawamoto, A., Tkebuchava, T., Yamaguchi, J., Nishimura, H., Yoon, Y.S., Milliken, C., *et al*. Intramyocardial transplantation of autologous endothelial progenitor cells for therapeutic neovascularization of myocardial ischemia. Circulation **107,** 461, 2003.
4. Rafii, S. Circulating endothelial precursors: mystery, reality, and promise. J Clin Invest **105,** 17, 2000.
5. Martin-Rendon, E., and Watt, S.M. Stem cell plasticity. Br J Haematol **122,** 877, 2003.
6. Duan, H.F., Wu, C.T., Wu, D.L., Lu, Y., Liu, H.J., Ha, X.Q., *et al*. Treatment of myocardial ischemia with bone marrow-derived mesenchymal stem cells overexpressing hepatocyte growth factor. Mol Ther **8,** 467, 2003.
7. Barbash, I.M., Chouraqui, P., Baron, J., Feinberg, M.S., Etzion, S., Tessone, A., *et al*. Systemic delivery of bone marrow-derived mesenchymal stem cells to the infarcted myocardium: feasibility, cell migration, and body distribution. Circulation **108,** 863, 2003.
8. Itescu, S., Kocher, A.A., and Schuster, M.D. Myocardial neovascularization by adult bone marrow-derived angioblasts: strategies for improvement of cardiomyocyte function. Heart Fail Rev **8,** 253, 2003.
9. Murayama, T., and Asahara, T. Bone marrow-derived endothelial progenitor cells for vascular regeneration. Curr Opin Mol Ther **4,** 395, 2002.

10. Kale, S., Karihaloo, A., Clark, P.R., Kashgarian, M., Krause, D.S., and Cantley, L.G. Bone marrow stem cells contribute to repair of the ischemically injured renal tubule. J Clin Invest **112,** 42, 2003.
11. Kocher, A.A. Bone marrow-derived stem cells for ischemic hearts. Wien Klin Wochenschr **115,** 77, 2003.
12. Orlic, D. Adult bone marrow stem cells regenerate myocardium in ischemic heart disease. Ann NY Acad Sci **996,** 152, 2003.
13. Orlic, D. Adult BM stem cells regenerate mouse myocardium. Cytotherapy **4,** 521, 2002.
14. Ingram, D.A., Mead, L.E., Tanaka, H., Meade, V., Fenoglio, A., Mortell, K., *et al*. Identification of a novel hierarchy of endothelial progenitor cells using human peripheral and umbilical cord blood. Blood **104,** 2752, 2004.
15. Ingram, D.A., Krier, T.R., Mead, L.E., McGuire, C., Prater, D.N., Bhavsar, J., *et al*. Clonogenic endothelial progenitor cells are sensitive to oxidative stress. Stem Cells **25,** 297, 2007.
16. Au, P., Daheron, L.M., Duda, D.G., Cohen, K.S., Tyrrell, J.A., Lanning, R.M., *et al*. Differential *in vivo* potential of endothelial progenitor cells from human umbilical cord blood and adult peripheral blood to form functional long-lasting vessels. Blood **111,** 1302, 2008.
17. Schechner, J.S., Nath, A.K., Zheng, L., Kluger, M.S., Hughes, C.C., Sierra-Honigmann, M.R., *et al*. *In vivo* formation of complex microvessels lined by human endothelial cells in an immunodeficient mouse. Proc Natl Acad Sci USA **97,** 9191, 2000.
18. Melero-Martin, J.M., Khan, Z.A., Picard, A., Wu, X., Paruchuri, S., and Bischoff, J. *In vivo* vasculogenic potential of human blood-derived endothelial progenitor cells. Blood **109,** 4761, 2007.
19. Shepherd, B.R., Jay, S.M., Saltzman, W.M., Tellides, G., and Pober, J.S. Human aortic smooth muscle cells promote arteriole formation by coengrafted endothelial cells. Tissue Eng Part A **15,** 165, 2009.
20. Melero-Martin, J.M., De Obaldia, M.E., Kang, S.Y., Khan, Z.A., Yuan, L., Oettgen, P., *et al*. Engineering robust and functional vascular networks *in vivo* with human adult and cord blood-derived progenitor cells. Circ Res **103,** 194, 2008.
21. Zuk, P.A., Zhu, M., Mizuno, H., Huang, J., Futrell, J.W., Katz, A.J., *et al*. Multilineage cells from human adipose tissue: implications for cell-based therapies. Tissue Eng **7,** 211, 2001.
22. Traktuev, D.O., Merfeld-Clauss, S., Li, J., Kolonin, M., Arap, W., Pasqualini, R., *et al*. A population of multipotent CD34-positive adipose stromal cells share pericyte and mesenchymal surface markers, reside in a periendothelial location, and stabilize endothelial networks. Circ Res **102,** 77, 2008.
23. Rehman, J., Traktuev, D., Li, J., Merfeld-Clauss, S., Temm-Grove, C.J., Bovenkerk, J.E., *et al*. Secretion of angiogenic and antiapoptotic factors by human adipose stromal cells. Circulation **109,** 1292, 2004.
24. Traktuev, D.O., Prater, D.N., Merfeld-Clauss, S., Sanjeevaiah, A.R., Murphy, M., Johnstone, B.H., *et al*. Robust functional vascular network formation *in vivo* by cooperation of adipose progenitor and endothelial cells. Circ Res **104,** 1410, 2009.
25. Ponec, M., El Ghalbzouri, A., Dijkman, R., Kempenaar, J., van der Pluijm, G., and Koolwijk, P. Endothelial network formed with human dermal microvascular endothelial cells in autologous multicellular skin substitutes. Angiogenesis **7,** 295, 2004.
26. Lilly, B., and Kennard, S. Differential gene expression in a coculture model of angiogenesis reveals modulation of select pathways and a role for Notch signaling. Physiol Genomics **36,** 69, 2009.
27. Ponce, M.L. Tube formation: an *in vitro* matrigel angiogenesis assay. Methods Mol Biol **467,** 183, 2009.
28. West, D.C., and Burbridge, M.F. Three-dimensional *in vitro* anglogenesis in the rat aortic ring model. Methods Mol Biol **467,** 189, 2009.
29. Nehls, V., and Drenckhahn, D. A novel, microcarrier-based *in vitro* assay for rapid and reliable quantification of three-dimensional cell migration and angiogenesis. Microvasc Res **50,** 311, 1995.
30. Ingram, D.A., Lien, I.Z., Mead, L.E., Estes, M., Prater, D.N., Derr-Yellin, E., *et al*. *In vitro* hyperglycemia or a diabetic intrauterine environment reduces neonatal endothelial colony-forming cell numbers and function. Diabetes **57,** 724, 2008.
31. Amyot, F., Camphausen, K., Siavosh, A., Sackett, D., and Gandjbakhche, A. Quantitative method to study the network formation of endothelial cells in response to tumor angiogenic factors. Syst Biol **152,** 61, 2005.
32. da Silva Meirelles, L., Sand, T.T., Harman, R.J., Lennon, D.P., and Caplan, A.I. MSC frequency correlates with blood vessel density in equine adipose tissue. Tissue Eng Part A **15,** 221, 2009.
33. Tang, W., Zeve, D., Suh, J.M., Bosnakovski, D., Kyba, M., Hammer, R.E., *et al*. White fat progenitor cells reside in the adipose vasculature. Science **322,** 583, 2008.
34. Miranville, A., Heeschen, C., Sengenes, C., Curat, C.A., Busse, R., and Bouloumie, A. Improvement of postnatal neovascularization by human adipose tissue-derived stem cells. Circulation **110,** 349, 2004.
35. Planat-Benard, V., Silvestre, J.S., Cousin, B., Andre, M., Nibbelink, M., Tamarat, R., *et al*. Plasticity of human adipose lineage cells toward endothelial cells: physiological and therapeutic perspectives. Circulation **109,** 656, 2004.
36. Grant, D.S., Tashiro, K., Segui-Real, B., Yamada, Y., Martin, G.R., and Kleinman, H.K. Two different laminin domains mediate the differentiation of human endothelial cells into capillary-like structures *in vitro*. Cell **58,** 933, 1989.
37. Iozzo, R.V., and San Antonio, J.D. Heparan sulfate proteoglycans: heavy hitters in the angiogenesis arena. J Clin Invest **108,** 349, 2001.
38. Handler, M., Yurchenco, P.D., and Iozzo, R.V. Developmental expression of perlecan during murine embryogenesis. Dev Dyn **210,** 130, 1997.
39. Cagliero, E., Roth, T., Roy, S., and Lorenzi, M. Characteristics and mechanisms of high-glucose-induced overexpression of basement membrane components in cultured human endothelial cells. Diabetes **40,** 102, 1991.
40. Albelda, S.M., Oliver, P.D., Romer, L.H., and Buck, C.A. EndoCAM: a novel endothelial cell-cell adhesion molecule. J Cell Biol **110,** 1227, 1990.
41. DeLisser, H.M., Christofidou-Solomidou, M., Strieter, R.M., Burdick, M.D., Robinson, C.S., Wexler, R.S., *et al*. Involvement of endothelial PECAM-1/CD31 in angiogenesis. Am J Pathol **151,** 671, 1997.

Address correspondence to:
Dmitry O. Traktuev, Ph.D.
Department of Medicine
Indiana University School of Medicine
975 W. Walnut St. IB441
Indianapolis, IN 46202

E-mail: tdmitry@iupui.edu

Received: September 21, 2009
Accepted: April 30, 2010
Online Publication Date: June 11, 2010